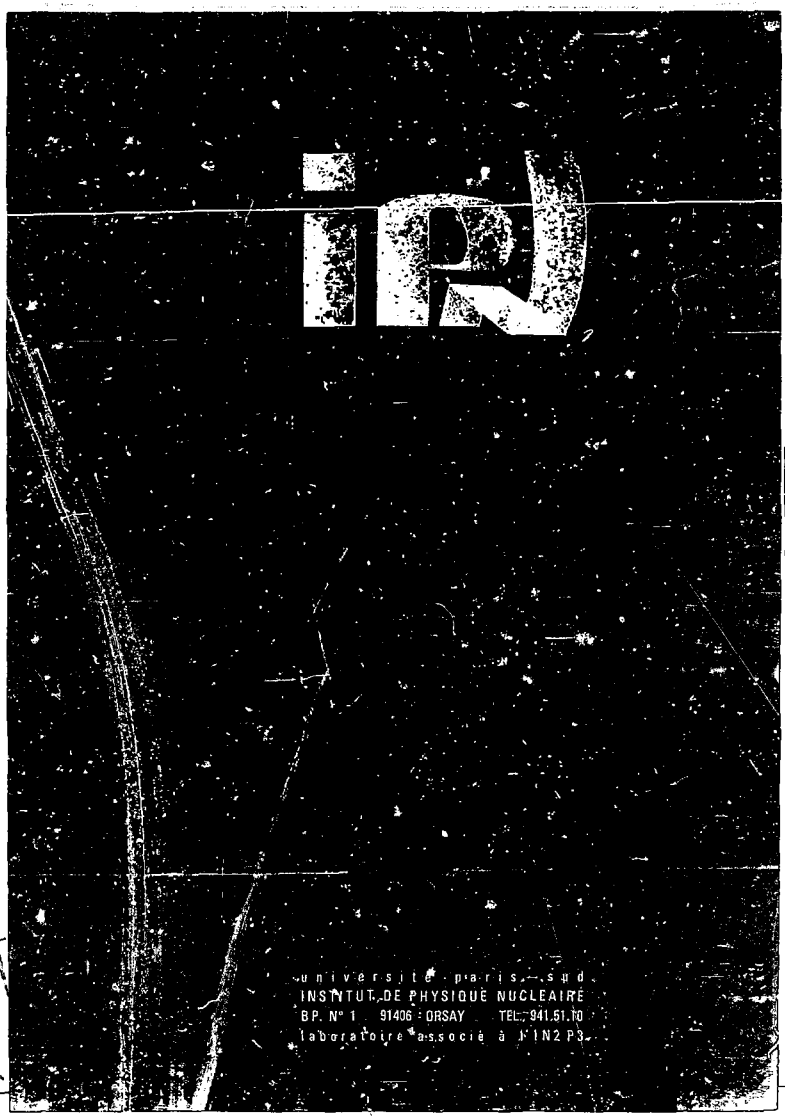

université paris-sud
INSTITUT DE PHYSIQUE NUCLEAIRE
B.P. N° 1 91406 ORSAY TEL. 941.61.70
laboratoire associé à l'IN2P3

Gamma-ray multiplicity measurements and Angular momentum transfer in Deeply Inelastic Collisions

Nils PERRIN and Jean PETER *

IPNO-RC-77-02
FR7701911

* Presented at the Winter School on Nuclear Physics, Zakopane (Poland), February 1977.

Gamma-ray multiplicity measurements and Angular momentum transfer in Deeply Inelastic Collisions

Nils PERRIN and Jean PETER

Institut de Physique Nucléaire, BP n°1, 91406 Orsay, France.

I - Introduction.

In the last few years, a great deal of experimental and theoretical work has been devoted to the study of deep inelastic collisions (DIC) (1-10). The fundamental reason is that these studies can provide informations on the interaction between two complex nuclei taken as two pieces of nuclear matter. Rather than the individual interactions between the nucleons, it is the macrophysical properties of the system that are concerned, such as the viscosity of the nuclear matter and the friction forces which act between the two interacting nuclei.

Up to now, experimental informations were mainly obtained from the characteristics of the final reaction products which are easily measured : kinetic energy, mass, charge, angular distribution and cross section. They all show that the outgoing channel has kept a strong memory of the entrance channel but for the kinetic energy and charge-to-mass ratios. Lately these measurements have been extended to the measure of the γ rays as a way to reach angular momentum transfer in DIC.

Disregarding the emission of light particles , the characteristics of DIC are the following.

1. A large part of the initial relative motion is transferred to other degrees of freedom up to a maximum value which is reached when the final relative motion is equal to the Coulomb repulsion plus centrifugal energy between the two fragments. These events correspond to the most inelastic collisions and are often called "relaxed" or "quasi-fission" events. They imply that during the collision, a composite system is formed, made of the two initial nuclei connected by a neck and having no relative velocity.

2. The masses and charges of the fragments remain in the general vicinity of the projectile and target masses and charges. Nevertheless, during the existence of the composite system, transfers of charges and masses occur.

The average mass differs from the initial one and the mass distribution broadens when the angle moves away from the grazing angle, indicating that the composite system lives a longer time. The rotation angle of the system before scission can be used as a "clock" to measure the decay time (from less than 10^{-21}s up to 10^{-20}s).

3. The angular distributions are strongly peaked. For the projectile-like products, they peak a bit forward of the grazing angle. Thus, when the grazing angle has a low value, they peak at very forward angles, and a part of the angular distribution reaches "negative" angles.

4. Near the grazing angle, a continuous distribution in kinetic energy, charge, mass and angle is observed from quasi-elastic transfer products to relaxed fragments. It indicates that the DIC are due to ℓ-waves just below ℓ_{gr} (ℓ-wave for grazing trajectories) (fig.1).

5. The relative importance of the deep inelastic cross section increases with the product Z_1Z_2 (projectile and target charges) and with the ratio of the incident energy to the entrance channel Coulomb barrier Ei/Vc. For light or medium-mass systems, the fusion cross section is large and the range of initial ℓ-waves contributing to deep inelastic collisions is rather narrow. For very heavy systems, the fusion cross-section vanishes and the range of ℓ-waves of DIC extends on a very broad range (fig.1 and table 1).

6. The average N/Z values of the fragments differ from those of the projectile and target nuclei (independently of the effect of subsequent deexcitation by particle emission).

The main features of these characteristics are reasonnably explained theoretically. Classical equations of motion including a dissipative term (friction) allow to reproduce the kinetic energy loss and angular distribution. The evolution of the mass distribution is explained by a diffusion process, based on the Fokker-Planck equation or master equation; the driving force is derived from the potential energy of the composite system. The N/Z values are those which minimize this potential energy (for a given N or Z).

But a question remains : what is the nature of the composite system ? Do the nuclei stick together to form a rigid body for a while, or do they keep some relative rotational motion ? The measurement of the angular momentum of the final fragments can help to answer this question.

Indeed, during the formation of the composite system, not only the relative motion is reduced by radial friction but also the value of the initial orbital angular momentum is reduced by tangential friction. Tangential friction can be decomposed into sliding friction, which acts to prevent mutual sliding, and rolling friction, which acts to prevent mutual rolling. At the beginning of the collision, the two nuclei slide on each other. The sliding friction force induces a rotation of the nuclei. When the two peripherical velocities are equal, the sliding friction force is reduced to zero. But during the rotational acceleration, rolling friction force has developped which tends to reduce the rotation. Finally the nuclei stick together and the system rotates as a rigid body (11-12).

The ratio of the transferred angular momentum $\Delta\ell$ to the initial orbital angular momentum ℓ_i (the spins of the target and projectile nuclei are neglected) depends on the stage of the continuous process described above which is reached when the two fragments separate. The experimental value of $\Delta\ell/\ell_i$ will indicate if the life time of the composite system is larger or smaller than the times necessary to reach the rolling or sticking situation.

Indeed, the rolling situation corresponds to a transfer of angular momentum $\Delta\ell_r$ independent of the mass ratio of the fragment : $\Delta\ell_r/\ell_i = 2/7$ for two spherical fragments. The maximum transfer of angular momentum is reached in the sticking situation :

$$\frac{\Delta\ell_s}{\ell_i} = \frac{J_H + J_L}{J_H + J_L + J_{orb}} \qquad (1)$$

where the numerator and denominator are the moments of inertia when the two nuclei are separated and when they are stuck together, respectively. J_H and J_L are the moments of inertia of the heavy and light final fragments relative to their rotation axis, and J_{orb} is the moment of inertia of these two fragments relative to the center of gravity (Huyghens theorem). J_H, J_L and J_{orb} depend on the shape of the composite system at the scission-point. Fig.2 illustrates this formula for a scission-point shape made of two tangent

spheres or deformed nuclei as a function of the mass ratio of the fragments. For spherical fragments, $\Delta\ell_s = \Delta\ell_r$ when the two fragments are equal; but the difference between $\Delta\ell_r$ and $\Delta\ell_s$ increases with the mass asymmetry (at the limit, $\Delta\ell_s/\ell_i = 1$ for complete fusion). It is thus better to study asymmetric projectile + target systems and/or look at very asymmetric final fragments couples (table I). The deformed case corresponds to ellipsoids elongated along the scission axis. Their deformation ($\beta = 0.3$) correspond to the value deduced from the quasi-fission kinetic energy of heavy systems. $\Delta\ell_s$ is smaller than for two spheres.

In the rolling situation, $\Delta\ell_r$ is shared between the two fragments in proportion to their radius :

$$\left(\frac{\Delta\ell_H}{\Delta\ell_L}\right)_r = \left(\frac{A_H}{A_L}\right)^{1/3} \qquad (2)$$

but in the sticking case, the heavy fragment is much more favored since $\Delta\ell$ is shared proportionnally to the moments of inertia:

$$\left(\frac{\Delta\ell_H}{\Delta\ell_S}\right)_S = \frac{A_H R_H^2}{A_L R_L^2} = \left(\frac{A_H}{A_L}\right)^{5/3} \qquad (3)$$

The measurement of $\Delta\ell_H/\Delta\ell_L$ would give an information on the stage reached in the DIC process. However, no such measurement have been made and we will discuss only in terms of $\Delta\ell/\ell_i$.

A large amount of energy and angular momentum has been transferred to the fragments of DIC. It is now assumed that the deexcitation of these fragments follows a pattern similar to the deexcitation of the compound nucleus.

I.1 - The compound nucleus deexcitation (13-20).

This process is now quite well known. The first step goes through particle emission, essentially evaporated neutrons for heavy fragments, which have a kinetic energy of a few MeV and carry away each approximately $1\hbar$ unit of angular momentum (13). When a point (fig.3) approximately 8 MeV above the Yrast line is reached there is not enough energy left to emit one more particle, and γ-ray emission which is much slower can now compete. At that point the nucleus has cooled off but still retains most of its initial angular momentum. γ emission starts with high energy statistical γ mostly E_1 in caracter emitted as a continuous spectra, until the nucleus is near enough to the Yrast line and decays then through stretched E_2 bands. These have to be numerous enough (>10) and with no connection one with another, because at that point the γ spectra is still continuous. These γ form a bump on the energy spectra, whose maximum lies at

$$E_\gamma = \frac{\hbar^2}{2\mathcal{J}_{rig}} \cdot (4I - 2) \qquad (4)$$

where J_{rig} is the rigid body moment of inertia. This bump is quite visible on fig.4 on the high energy statistical γ ray spectra. Angular correlation measurements are coherent with the assigned multipolarity of the γ (fig.4). When the Yrast line is finally reached the nucleus emits discrete lines characteristic of the ground base band, and it is through these lines that the fragment can be identified. Now we have seen that most of the angular momentum is carried away by γ emission. It is then possible to reach the initial momentum by counting the number of these γ rays (this number M_γ is called the γ multiplicity) and multiply by their average multipolarity (approximately 10% of these γ are E_1, 90% E_2, higher multipolarity are absent, because feeding time have been measured to be too short (10 pico seconds) to permit higher multipolarity emission).

Multiplicity measurements are done most simply through coincidence between a particle detector and a γ ray counter. The number of these coincidence is given by

$$N_c = N_S[1 - (1-\Omega_\gamma)^{M_\gamma}] \qquad (5)$$

where N_S is the number of reactions as counted by the heavy-ion detector, Ω_γ is the total efficiency of the γ ray detector including solid angle, and M_γ the average multiplicity. To the first order because Ω_γ is rather small we have

$$\frac{N_c}{N_S} = M_\gamma \, \Omega_\gamma \qquad (6)$$

It is important to note that the multiplicity thus measured is only an average multiplicity per event. We have no information on the spread of that multiplicity. This will proove to be important when we discuss the anisotropy of the γ emission. However it could be possible with a multi-counter arrangement to measure (18) the distribution of the multiplicity around the average value, more exactly measures the higher order momenta of this distribution. This would give important information on the mecanism that gives an isotropic γ ray distribution.

The angular momentum carried away by the γ is thus $M_\gamma \times$ the average multipolarity which is near to 2. To go back to the original momentum as many units of $\hbar$ as neutrons have been emitted are added.

We must stress here that the C.N. deexcitation scheme is not at all the whole picture. There are at least two points which deviate from this scheme. Firstly no account has been taken of the momentum that may be carried away by one or more energetic particle emitted at the beginning (n,p,α). This may be important as indications have been given for the emission of energetic α early in the reaction. Secondly, while the momentum in C.N. formation is aligned perpendicular to the beam direction and has been measured so, in DIC the momentum transferred is polarized perpendicular to the reaction plane or should be. The fact that it is not is an important difference that is not well understood. An explanation of this fact can be obtained through the study of multiplicity measurement in fission.

I.2 - Prompt gamma-ray emission in fission (21-26).

When a heavy nucleus undergoes spontaneous or thermal neutron induced fission, its fragments emit several gamma-rays in less than 1 us. Accurate measurements have been made for even-even fissionning nuclei ^{252}Cf, $^{233}U+n_{th}$, $^{235}U+n_{th}$, $^{239}Pu+n_{th}$.

If no specific fragment is selected, the gamma-ray energy spectrum is continuous with a maximum around 600 keV (21-23) and a high-energy tail which was measured up to 20 MeV (24-25). This tail, which can be attributed mainly to E1 transition, is a very low percentage of the total spectrum. The angular distribution is peaked in the flight direction of the fragment, which indicates that the fragments are polarized in the plane perpendicular to the flight direction. They are emitted in less than 10^{-12}s. It is concluded that they are mainly E2 transitions. The above results were clearly confirmed by studies of specific gamma-rays (26) (anisotropy $W(0°)/W(90°) = 1.5$, direct observation of E2 transitions).

The number of gamma-rays emitted by each fragment is proportionnal to its excitation energy, and thus the variation of N_γ as a function of the fragment mass reproduces the saw tooth curve observed for the number of emitted neutrons. The total number is around 7 for the nuclei listed above (fig.6), and the total angular momentum is $\sim 15\ \hbar$.

The "creation" of angular momentum in the fission process is attributed to the bending mode of deformation, and also to twisting and wriggling modes. Can this creation also occur in the last stage of the DIC process, when the two nuclei begin to separate ? The characteristic times associated with these modes are $\sim 10^{-21}$s (27). This is the life-time of the composite system for relaxed or quasi-fission events, therefore these modes could be exicted. But what is the value of this angular momentum ? This is difficult to answer. In DIC the temperature of the composite system is greater than 1 MeV, and the value of N_γ in high energy induced fission should be used rather than that of spontaneous or thermal neutron induced fission. But this value has not yet been measured (data are being processed on the gamma multiplicity of fission of Ar+Au (33).

We can simply expect that an angular momentum ℓ_{bd} of several $\hbar$ is "created" in the fragments, independently of $\Delta\ell$ transferred from the orbital angular momentum. Its direction is perpendicular to the direction of the fragments, but not necessarily parallel to the orbital angular momentum direction. This would spread out the distribution of the multiplicity without changing much the average value. This effect could be measured by a multi-counter experiment.

II - Gamma-ray multiplicity measurements in DIC.

II.1 - Studied systems (28-36).

Seven systems have been studied. They are listed in table 1 together with the ranges of initial ℓ-waves which contribute to relaxed or quasi-fission events (between ℓ_{crit} and ℓ_{DIC}) and those contributing to partially

Projectile	Target	E_{inc} labo	ℓ_{crit} fusion	ℓ DIC	ℓ_{gr} reactions	θ_{gr} labo	$\theta_{measured}$ labo	Mass ratio initial	Mass ratio final studied	Ref.
^{16}O	^{nat}Ni	96	42	49		17°	30°-70°	3.7	3.7, 5.2	28
^{14}N	^{93}Nb	120	44		60	20°	40°	6.6	4.4 - 15	30
^{20}Ne	^{nat}Ni	175	57±7	70		22°	25°,35°,90°	5.4	1.4 - 8.5	32
^{40}Ar	^{58}Ni	280	74±5	98±7	105	18°	16°-32°	1.5	1 - 8	29
^{40}Ar	^{197}Au	227	68±5	76±5	88	82°	50°	.5	1 - 7	33
^{63}Cu	^{197}Au	365	≤ 25	75±7	95	110°	50°,80°,100°	3.1	1 - 5.5	33
^{63}Cu	^{197}Au	443	≤ 61	175±8	195	70°	35°,49°		1 - 3.1	31
^{84}Kr	^{197}Au	600	< 50 ?	∿220	250	∿40°	30,40,55,70°	2.3		34

Table 1. Systems studied for gamma-ray multiplicities in DIC.
ℓ_{crit} is the maximum ℓ-value for which complete fusion occurs.
Relaxed DIC or quasi-fission occur between ℓ_{crit} and ℓ_{DIC}.

damped collisions (between ℓ_{DIC} and ℓ_{gr}). These values of ℓ_i were calculated with simple sharp cut-off approximations, assuming that complete fusion occurs between ℓ=0 and ℓ_{crit}. These experiments are referred thereafter by the projectile and target symbols and incident laboratory energy (O Ni 96..).

II.2 - Experimental techniques.

As we have seen multiplicity is measured through

$$N_c/N_s = M_\gamma \cdot \Omega$$

The fragments can be identified simply by their kinetic energy provided the range of masses associated with a given kinetic energy is known by previous experiments (Cu Au 443). More precise informations are obtained when the charge (*O Ni 96, N Nb 120, Ne Ag 175, Ar Ni 280 with the ΔE-E telescope* technique) or the mass (Ar Au 227, Cu Au 365, fig.6, with the time-of-flight technique) is measured for each event in addition to the kinetic energy.

In most experiments γ counters are 3x3"NaI(Tl) they are shielded by copper and/or lead so that the efficiency varies as little as possible over the range of considered energy (0.5 to 6 MeV). Usually a bias is placed at 200 to 600 keV to suppress diffused and low energy γ (fig.7). This threshold is below the energy where continuum transition are expected, this can be tested by changing threshold value and comparing the corresponding multiplicity. As NaI counters are sensible to neutrons (neutron efficiency is of the order of 1 to 5% that for γ rays depending on threshold value (44) they are placed far from the target to be able to discriminate the neutrons by a time-of-flight method. With a time resolution of 6 ns, 60 cm is a good choice. It is seen (fig.8) that especially for backward angles no neutron discrimination is necessary. For example in the Ar+Au 227, Cu + Au 365 experiment, we placed the counters at 30cm which enabled us to check that neutron were not important and to give a possible evaluation though separation was not complete.

In O Ni 96, the distance was only 15cm, thanks to the 3ns resolution obtained. No discrimination could be made in N Nb 120, since the distance was 6cm, but the rate of neutrons was determined to be less than 10% by comparing measurements made with and without a Pb absorber in front of the crystal.

The γ spectra obtained must then be unfolded to give the number of γ-rays versus energy (fig.4). This can be done using Mollenauer code (35). This procedure is rather heavy and requires careful calibration of the detectors with standard sources. As one sees, the procedure to measure angular momentum of the fragments is rather painfull and accuracy is at most rather poor for absolute measurements. However relative values of multiplicity can be well relied on, and for example the variation of multiplicity with fragment energy is very sensitive.

II.3 - Variation of M_γ with the energy relaxation.

The variation of M_γ with the degree of relaxation of the kinetic energy has to be studied for given masses of the final fragments, since M_γ also varies with the mass ratio. In all works where this precaution is taken M_γ is found to increase with the inelasticity. This is not surprising since

$\Delta\ell$ is low in quasi-elastic reactions and gradually increases for, ℓ-waves below ℓ_{gr}, when the nuclei interpenetrate and the interaction lasts a longer time allowing sliding and rolling friction to act.

Figures 9 to 11 clearly show that in N Nb 120 (fig.9), M_γ increases rapidly and continuously when the degree of inelasticity increases. In Ar Ni 280 (fig.10), the increase is large for the first 30 MeV and then much slower. The same behaviour is observed in Cu Au 443 (fig.11) for the kinetic energy region of the average final mass ~63. The maximum value corresponds to quasi-fission events.

It is clear that in the fast surface interactions which lead to quasi-elastic transfers or partially-damped collisions, the tangential friction force is not strong and acts a short time, allowing only a partial ℓ-transfer. Maximum $\Delta\ell$ values are found in "relaxed" or "quasi-fission" events and we will further on restrict ourselves to these events.

III - Transferred angular momentum in DIC (relaxed events).

III.1 - Relation between M_γ and $\Delta\ell_{exp}$.

The relationship between the measured M_γ and the total intrinsic angular momentum of the fragments $\Delta\ell_{exp}$ is not at all straightforward. We have to know the multipolarity of these γ, take into account that some γ may escape the coincidence time window of the experiment (10 ns) and finally add the angular momentum carried away by evaporated particles.

These problems are similar to those encountered for the interpretation of multiplicities of compound nuclei and fission fragments. All authors rely on the results obtained in these two cases for nuclei in the vicinity of those obtained in DIC. This similarity is especially useful for the knowledge of the multipolarity, since no special measurements have been made on that point. The anisotropy of the angular distribution relative to the reaction plane could give directly this information but, as discussed later, the angular distribution is strongly perturbed. The shapes of the energy spectra are quite similar (fig.4 and 7) : the high energy part is due to statistical dipole and quadrupole radiations; the low energy bump is due to stretched E2 Yrast transitions. The maximum Yrast energy calculated with the formula (4) is consistent with the upper value of the bump (fig.7).

The angular momentum carried by 1 evaporated neutron is again taken to be $\hbar$ according to theoretical calculations (13). Evaporated alpha-particles can carry much more momentum but the precise value is not known and it is better to study nuclei which evaporate few alpha-particles and to check that experimentally.

We will examine how these problems were solved in the different works reported here :

- O Ni 96 - The multiplicity of alpha-particles emitted in coincidence with DIC products was measured and found to be low (36) : 0.1 and 0.2

respectively for final fragments O and C, including alpha-particles emitted by the composite system. From results obtained for compound nuclei of similar excitation energy and angular momenta, the multipolarity is taken to be 2 and the angular momentum carried away by particles is proportionnal to the excitation energy through the factor 3ħ/16 MeV (that corresponds to $\sim 1.8\hbar$ per neutron rather than $\hbar$). Thus $\Delta\ell_{exp} = 2 M_\gamma + E^* 3/16 = 3$ MeV for relaxed events.

- N Nb 120 - The same conclusions were experimentally obtained for the number of emitted alpha-particles (37). The angular momentum carried away by particles is taken into account by using a multiplication factor greater than 2 : $\Delta\ell_{exp} = 2.4\ M_\gamma$.

- Ne Ag 175 - Comparison with similar compound nuclei leads to estimate a balance between a few dipole gamma-rays and some particle emission that carries angular momentum, thus $\Delta\ell_{exp} = 2\ M_\gamma$.

- Ar Ni 280 - The number of coincident alpha-particles is large : 1.5 (29,9). 10 to 12 nucleons can be evaporated, thus carrying an important angular momentum.

- Cu Au 443 - For the similar system $^{84}Kr+^{197}Au$ at 718 MeV, the numbers of coincident alpha-particles and protons are 0.23 and 0.15 respectively (38), and they are neglected. A number of 12 evaporated neutrons is calculated, thus carrying away $12\hbar$. The number of statistical gamma-rays, which are mostly E1, is 10% of the total. Thus the average multipolarity is 1.9 and $\Delta\ell_{exp} = 1.9\ M_\gamma + 12 = 2.4\ M_\gamma$ for quasi-fission events.

It is clear that the missing information on the angular momentum carried away by evaporated alpha-particles is a serious drawback of these studies. Furthermore the value attributed to evaporated neutrons is only an estimate. The factor applied to M_γ to obtain $\Delta\ell_{exp}$ varies from 2 to 3, and the error on the value of $\Delta\ell_{exp}$ is of the order of 20% (independently of statistical errors).

III.2 - Sliding, rolling or sticking ?

Now we can compare $\Delta\ell$ to the calculated possible values. $\Delta\ell/\ell$ depends on three quantities at the scission-point : the mass ratio of the final fragments, their deformation and the degree of cohesion of the composite system : fig.2. Our main purpose is to determine the degree of cohesion. But what do we know about the two other quantities ?

First , the mass ratio (or charge ratio) is directly measured with a small error due to particles evaporated from the fragments. Secondly, the deformation can be deduced from the Coulomb repulsion at the scission-point E_C since, for a given couple of fragments M_H, M_L issued of relaxed events, assuming that the relative velocity at the scission-point is zero :

$$E_C(M_H/M_L) = E_K(M_H/M_L, \ell) - E_{R_{orb}}(M_H/M_L, \ell_f) \qquad (7)$$

where E_K is the measured kinetic energy and $E_{R_{orb}}$ the orbital rotationnal energy at the scission-point. But $E_{R_{orb}}$ also depends on the degree of cohesion and on ℓ_i. For heavy systems, $E_{R_{orb}}$ is small(10-30 MeV) compared to E_K

(160-280 MeV) and E_C is determined with a small uncertainty. It is ∿ 20% lower than V_C thus indicating a prolate deformation ? $E_{R_{orb}}$ is small compared to E_C and the precise value of the moment of inertia is not necessary. A semi-axis ratio of ∿ 1.3 is calculated. For medium-mass systems, $E_{R_{orb}}$ may reach half of E_C and the deformation cannot be well determined ; available data are consistent with the value of 1.3.If the velocity at the scission-point is not zero,the elongation is larger.

In $\Delta\ell/\ell$, ℓ is the total angular momentum at the scission, equal to the initial one, ℓ_i,or smaller if particle emission occurs before the scission-point. Due to lack of information, we calculate $\Delta\ell_C$ assuming $\ell = \ell_i$. But we must remember that the emission of particles carrying away a large angular momentum from the composite system can be responsible for a difference between $\Delta\ell_C$ and $\Delta\ell_{exp}$ (the emission of such particles from the fragments also diminishes $\Delta\ell_{exp}$.)

Variation of $\Delta\ell_{exp}$ with the mass asymmetry at different angles.

The common feature of the five medium-mass systems studied is a small value of θ_{gr} (table 1) due to a large E_i/V_C ratio. Most DIC orbits go through 0°. The decay time of the composite system increases with θ, for $\theta > \theta_{gr}$. For these systems M_γ of relaxed events was found to increase with the mass asymmetry M_H/M_L.

For O Ni 96,the relative variation of $\Delta\ell_{exp}$ between final masses 12 and 16 is that calculated with the sticking hypothesis, but the absolute values of 15ħ and 12ħ respectively are in agreement with the rolling value of 13ħ rather than with the sticking values of 23 and 20 (spherical fragments). For a given mass, M_γ of relaxed events slowly increases with θ (fig.16), i.e. with decay time of the composite system, but it has not yet reached the rigid body limit at 70°.

A similar behaviour is observed for Ne Ag 175 (fig.13), but here the time corresponding to the largest angle is sufficient to reach the rigid body. 25° and 35° correspond to short decay times, and the values obtained there agree with the rolling situation, but, as pointed out by the authors, it does not imply the existence of "rolling". It may be that the decay times is such that $\Delta\ell/\ell$ chances to be 2/7. For longer times, i.e. larger angles, $\Delta\ell/\ell$ continues to increase and reaches the sticking limit before or at 90°.

For the other cases , we do not know the variation versus the angle. $\Delta\ell/\ell$ increases with M_H/M_L. It implies that the composite system has over-reached the rolling stage. If we trust the absolute values of $\Delta\ell_{exp}$, these results are in agreement with the sticking case. For Ar Ni 280, if the ∿ 12 emitted nucleons carry away 12ħ, $\Delta\ell_{exp}/\ell_i$ reaches 2/7 for a mass ratio ∿ 1, but the slope of $\Delta\ell_{exp}$ against the mass asymmetry is definitely too low as compared with the sticking hypothesis and seems to indicate a situation slightly after rolling (fig.14).

For the heavy systems, the interpretation of the data is not so easy. A broad range of ℓ-waves contribute to the "relaxed" or "quasi-fission" component (fig.1), and a $\Delta\ell$ value at a given angle θ is affected by the average value of ℓ_i decaying at this angle as well as by the degree of cohesion.On the other hand, we expect to get informations on the deflection function $\theta(\ell_i)$. That

will be less ambiguous for systems studied at $E_i/V_C < 1.5$ where orbiting is negligible and the problem of decomposition into positive and negative branches is avoided.

Results are published only for Cu Au 443. They are summarized in fig.15 where we have taken $\Delta\ell_{exp} = 2M_\gamma$. If particle emission is taken into account, the absolute value of $\Delta\ell_{exp}$ is in agreement with the sticking hypothesis. But M_γ increases less with the mass asymmetry than expected with this hypothesis.

At 49° a slight decrease of M_γ with the mass asymmetry is even observed. The values are higher at 35° than at 49°.

These results suggest the following process : 1) The composite system reaches the rigid body situation very close to the grazing angle, unlike the light systems. Indeed, the volume of overlap is larger and the friction forces are stronger. Moreover, the rotationnal velocities of the composite system are lower than for the medium-mass systems studied here and the time necessary to reach the rigid body corresponds to a smaller rotation angle. 2) A broad range of ℓ-waves decays at a given θ. For the high ℓ-waves, a large mass transfer towards symmetry occurs, because the driving force derived from the potential energy tends to reduce the mass asymmetry (43) and this force increases with ℓ (44). Thus the low mass asymmetry exit channel corresponds on average to large ℓ_i and, although $\Delta\ell/\ell_i$ is small, $\Delta\ell$ can be equal or even greater than the $\Delta\ell$ for small mass transfer but issued from lower ℓ_i-values. These views are supported by the preliminary data of recent experiments (34).

These results show that the events leading to nearly equal masses are not issued from fission after complete fusion. ℓ_{crit} is well below the upper limit deduced from the study of mass distributions as shown in fig.1 (40). It even could be zero. More will be learned by adding the data on $\Delta\ell$ to the data already obtained on the mass, charge and kinetic energy distributions at every angle. In the rigid body configuration, relations (1) and (7) allow to obtain ℓ_i and the semi-axis ratio of the fragments at the scission-point. That require precise determinations of E_K and $\Delta\ell$.

Another question which has not yet been considered is the possibility of additional angular momentum in the fragments due to the bending mode. If the direction of this added angular momentum ℓ_{bd} is not correlated to ℓ_f but perpendicular to the direction of motion of the fragments, then the average resulting angular momentum is $\Delta\ell_C = (\Delta\ell^2+\ell_{bd}^2)^{1/2}$. $\Delta\ell_{bd} \simeq \Delta\ell$ if $\ell_{bd} << \Delta\ell$. For heavy systems, the data obtained in fission indicate it is so. But the second moment of the distribution $\Delta\ell$ is increased, and that could be a way of checking the value of ℓ_{bd}. ℓ_{bd} has another consequence which will be discussed now.

III-4 Angular distribution of gamma-rays.

One advantage of the DIC as compared to the compound nucleus is the knowledge of the direction of the orbital angular momentum ℓ_i, since the direction of the fragments define the reaction plane.

In most experiments and as expected, the counting rate of the gamma detectors in the reaction plane were found to be equal. In some cases (NNb 120, Cu Au 443), the distribution was also measured in the direction perpendicular to the reaction plane.

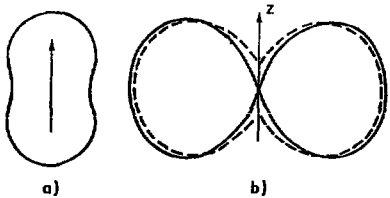

Fig. 17- Theoretical anisotropy for γ ray emission by an initial state with 60ħ angular momentum aligned along the Z direction. a) ℓ=1 stretched transition. b) stretched E2 transition. The dotted line corresponds to an initial angular momentum width of 12ħ. From ref. 42.

If the emission is mostly stretched E_2 from polarised nuclei, a very low counting rate is expected in this direction (fig. 17). Surprisingly it was found to be 80-95% of the counting rate in the reaction plane.

Now the angular distribution of E1 transitions is maximum in this direction, but their percentage is low (≈10%). What can this loss of alignment be due to ?

First, the evaporation of neutrons before gamma-ray emission leads to some disalignment, but not large enough. Alpha-particle emission could have the same effect by modifying either the direction of ℓ_i (emission from the composite system) or the direction of $\Delta\ell_h$ and/or $\Delta\ell_L$ (evaporation from the fragments). In the studied cases, the number of alpha-particles is much lower than 1 per DIC event. We are led to consider the effect of the additionnal angular momentum ℓ_{DIC}. If we assume that its direction is not correlated to that of $\Delta\ell$, the direction of the resulting $\Delta\ell_c$ varies of $\pm$ Arc sin(ℓ_{bd} /$\Delta\ell$).

For the case of CuAu 443, we can use the results of fission to estimate ℓ_{bd}. If the last stage of the DIC process is similar to fission in the stage from saddle-point to scission-point, then the results obtained for fission of ^{235}U or ^{252}Cf can be used for the composite system $^{260}108$.

The striking point in figure 5 is that M_γ does not depend on the mass asymmetry. We can thus estimate that, even for the very asymmetric case $M_H/M_L = 3.1$, ℓ_{bd} can be of the order of 15ħ. The maximum value of $\Delta\ell$, calculated with the sticking hypothesis for prolate fragments, is 43ħ. The direction of the resulting $\Delta\ell_c$ varies on a range of ±30° which reduces very much the anisotropy*.

*Note : the angular momenta due to the bending mode in the two fragments are equal (and their directions are opposite) $\ell_{bdH} = \ell_{bdL} = \ell_{bd}/2$. Since $\Delta\ell_L < \Delta\ell_H$, ℓ_{bdL} can be equal or greater than $\Delta\ell_L$ and the anisotropy in the direction out-of-plane is completely destroyed for the γ-rays emitted from the light fragment. Moreover, for these γ-rays, an anisotropy should be produced in the reaction plane : maximum in the direction of the light fragment.

Conclusion

The situation is not quite as clear as we should like. The data are not complete and it is difficult to get the absolute values of $\Delta\ell_{exp}$. That means that the relative variation of $\Delta\ell_{exp}$ with the angle and with the final mass asymmetry are the most reliable. A very good information would be the ratio $\Delta\ell_{\parallel}/\Delta\ell_{\perp}$, since it depends only on the degree of cohesion. Not very clear is also the question of the "creation" of intrinsic angular momenta in the fragments due to the DIC process itself. However it could be useful to explain the low anisotropy of the gamma-rays angular distribution.

For a given mass asymmetry and angle, the transferred angular momentum increases with the degree of inelasticity of the collision. For medium-mass systems, the cohesion of the composite system varies continuously from the rolling to the sticking situation when its decay time increases. The rigid body is obtained for a small part of the DIC (relaxed events) cross section. For heavy systems, the sticking case seems to be much more common, which will allow to extract information on the deflection function and the fusion cross section.

The rigid body situation is obtained only when the time of the composite system is of the order of a few 10^{-21}s. This time is larger than the times needed for N/Z or kinetic energy relaxation, but shorter than the relaxation time of the mass asymmetry degree of freedom.

We are grateful to F.S. Stephens and L.G. Moretto for the authorization to use their data before publication. Thanks are due to our colleagues at Orsay for fruitful discussions and careful reading of the manuscript : M.Berlanger, M.A. Deleplanque, C. Gerschel, J. Galin, F. Hanappe, N. Ishihara, C. Ngô, D. Paya, Y. Sugiyama, B. Tamain, L. Valentin.

References

1. R. Kaufman and R. Wolfgang, Phys. Rev. 121 (1961) 192.
   H. Kumpf and E.D. Donetz, JETP (USSR) 44 (1963) 798, Sov. Phys. JETP 17 (1963) 539.
2. G.F. Gridnev, V.V. Volkov, J. Wilczynski, Nucl. Phys. A142 (1970) 385.
   A.G. Artukh, G.F. Gridnev, V.L. Mikheev, V.V. Volkov, J. Wilczynski, Nucl. Phys. A215 (1973) 91.
3. J. Galin, D. Guerreau, M. Lefort, J. Péter, X. Tarrago, R. Basile, Nucl. Phys. A159 (1970) 461.
4. M. Lefort, C. Ngô, J. Péter, B. Tamain, Nucl. Phys. A216 (1973) 166.
   F. Hanappe, M. Lefort, C. Ngô, J. Péter, B. Tamain, Phys. Rev. Lett. 32 (1974) 738.
5. L.G. Moretto, D. Heunemann, R.C. Jared, R.C. Gatti, S.G. Thompson, Third Symposium on Fission, Rochester (1973) paper SM 174/75, IAEA Vienna.
   K.L. Wolf, J.P. Unik, J.R. Huizenga, J. Birkelund, H. Freiesleben, V.E. Viola, Phys. Rev. Lett. 33 (1974) 1105.
6. M. Lefort, Nukleonika 21 (1976) 111.
7. V.V. Volkov, Nukleonika 21(1976) 53.
8. J. Péter, Conference Physics of Tandem, Trieste (1976), Orsay Report IPNO-RC-76-02.
9. J. Galin, J. Physique, Colloque C5, 37 (1976) C5-83.
10. L.G. Moretto and R. Schmitt, J. Physique, Colloque C5, 37 (1976) C5 109.
11. C.F. Tsang, Physica Scripta 10A (1974) 90.
12. J.P. Bondorf, Proceedings Internat. School of Physics, Varenna (1974).
13. J.R. Grover and J. Gilat, Phys. Rev. 157 (1967) 802 ; 157 (1967) 814 ; 157 (1967) 823.
14. J.F. Mollenauer, Phys. Rev. 127 (1962) 867.
15. P.O. Tjøm, F.S. Stephens, R.M. Diamond, J. de Boer, W.E. Meyerhoff, Phys. Rev. Lett. 33 (1974) 593.
16. E. der Mateosian, O.C. Kistner, A.W. Sunyar, Phys. Rev. Lett. 33 (1974) 596.
17. J.O. Newton, J.C. Lisle, G. D. Dracoulis, D.R. Leigh, D.C. Weisser, Phys. Rev. Lett. 34 (1975) 99.
18. G.R. Hagemann, R. Broda, B. Herskind, M. Ishihara, S. Ogaza, Nucl. Phys. A245 (1975) 166.
19. R.S. Simon, M.V. Banaschik, P. Colombani, D.P. Soroka, F.S. Stephens, R.M. Diamond, Phys. Rev. Lett. 36 (1976) 359.
20. R.M. Diamond, Nukleonika 21 (1976) 29.
21. P. Armbruster, H. Labus, K. Reichelt, Z. f. Natur. 26A (1971) 512.
22. F. Pleasonton, R.L. Ferguson, H.W. Schmitt, Phys. Rev. C6 (1972) 1023.
23. F. Pleasonton, Nucl. Phys. A213 (1973) 413.
24. H.W. Sobel, A.A. Hruschka, W.R. Kropp, J. Lathrop, F. Reines, M.F. Crouch, B.S. Meyer, J.P.F. Sellschop, Phys. Rev. C7 (1973) 1564.
25. F.S. Dietrich, J.C. Browne, W.J. O'Connell, M.J. Kay, Phys. Rev. C10 (1974) 795.
26. A. Wolf and E. Cheifetz, Phys. Rev. C13 (1976) 1952.
27. J.R. Nix, W.J. Swiatecki, Nucl. Phys. 71 (1965) 1.
28. R. Albrecht, W. Dünnweber, G. Graw, H. Ho, S.G. Steadman and J.P. Wurm, Phys. Rev. Lett. 34 (1975) 1400.
29. R. Albrecht, B.B. Back, R. Bock, B. Fisher, A. Gobbi, K. Hildenbrand, W. Kohl, U. Lynden, I. Rode, H. Stelzer, G. Auger, J. Galin and J.M. Lagrange, Contribution to the Symposium on Gross Properties of Nuclei IV, Hirschegg, Austria, (1976) AED-CONF-76-015-000, p. 152, and to the European Conference on Nuclear Physics with Heavy Ions, Caen (1976) p. 167.
30. M. Ishihara, T. Numao, T. Fukuda, K. Tanaka and T. Inamura, Institut of Physical and Chemical Research, Wako-Shi, IPCR-Cyclotron Report 35, Contribut. to Argonne Symposium (1976).

31. M. Berlanger, M.A. Deleplanque, C. Gerschel, F. Hanappe, M. Leblanc, J.F. Mayault, C. Ngô, D. Paya, N. Perrin, J. Péter, B. Tamain and L. Valentin, J. Phys. Lett. (1976).
32. P. Glässel, R.S. Simon, R.M. Diamond, R.C. Jared, I.Y. Lee, L.G. Moretto, J.O. Newton, R. Schmitt and F.S. Stephens, preprint (1977).
33. M. Berlanger, M.A. Deleplanque, C. Gerschel, F. Hanappe, M. Ishihara, C. Ngô, D. Paya, N. Perrin, J. Péter, B. Tamain, L. Valentin, S. Yasuharu ; work in progress.
34. L.G. Moretto, R.M. Diamond, F.S. Stephens, P. Glässel, R. Simon et al., Work in progress.
35. J.F. Mollenauer, Lawrence Berkeley Laboratory Report, UCRL-9748 (1961).
36. A. Albrecht, C. Bercks, W. Dunnweber, G. Graw, H. Ho, J.P. Wurm, B. Disdier, V. Rauch and F. Scheibling, Contribution to the European Conference on Nuclear Physics with Heavy Ions, Caen (1976) p. 159.
37. M. Ishihara, H. Kamitsubo, T. Shimoda, F. Fukuda, T. Motobayashi, T. Ohi and I. Kohno, Contribution to the European Conference on Nuclear Physics with Heavy Ions, Caen (1976) p. 157.
38. D. Benson, G. Catchen, L. Kowalski, D. Logan, N. Lee, J. Miller, U.N. Singh, J. Alexander, T. Debiak and M. Guidry, preprint (1976).
39. B. Gatty, D. Guerreau, M. Lefort, X. Tarrago, J. Galin, B. Cauvin, J. Girard, H. Nifenecker, Nucl. Phys. A253 (1975) 511.
40. J. Péter, C. Ngô, F. Plasil, B. Tamain, M. Berlanger, F. Hanappe, Nucl. Phys. (to be published).
41. F. Hanappe et M.A. Deleplanque, C.R. Session d'Etudes de Physique Nucléaire, La Toussuire, published by Institut de Physique Nucléaire, Lyon.
42. C. Gerschel, Comptes-rendus Colloque franco-japonais de Spectroscopie Nucléaire et Réactions Nucléaires, Dogashima, Septembre 1976.
43. C. Ngô, J. Péter, B. Tamain, M. Berlanger, F. Hanappe, Nucl. Phys. A267 (1976) 181.
44. T.Inada, J. Nucl. Sci. and Technology 5 (1968) 287.

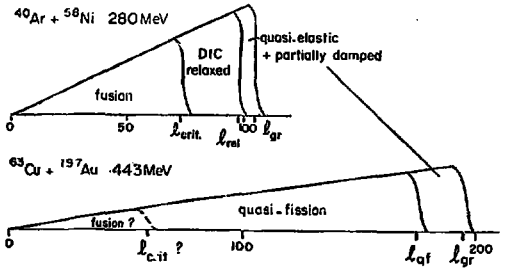

Fig.1. Windows of initial ℓ-waves contributing to the different reactions for a medium-mass and a very heavy systems (after ref.39-40). For the heavy system, it is not clear whether the low ℓ-waves contribute to complete fusion or to relaxed collisions (quasi-fission).

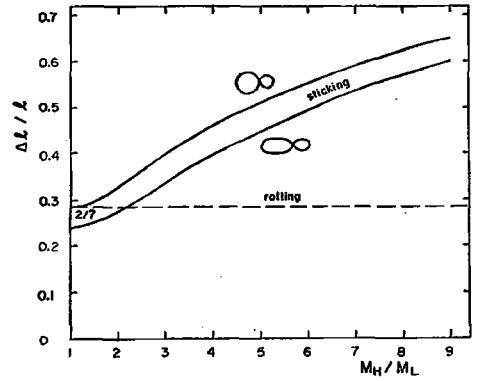

Fig.2. Proportion of the total angular momentum ℓ transferred into intrinsic moments of the final fragment Δℓ versus the mass ratio of the fragments. Any value up to that of the sticking can be actually reached. The sticking value is calculated for two configurations at the scission-point : tangent spheres and tangent prolate ellipsoids of semi-axis ratio 1.3.

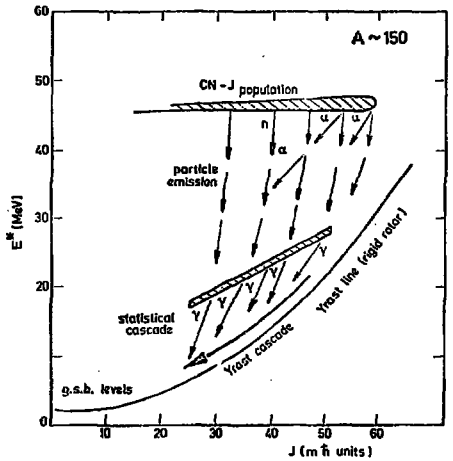

Fig.3. Schematic diagram of the de-excitation of a compound nucleus (mass 150) with a high angular momentum. *From* ref.20 and 41.

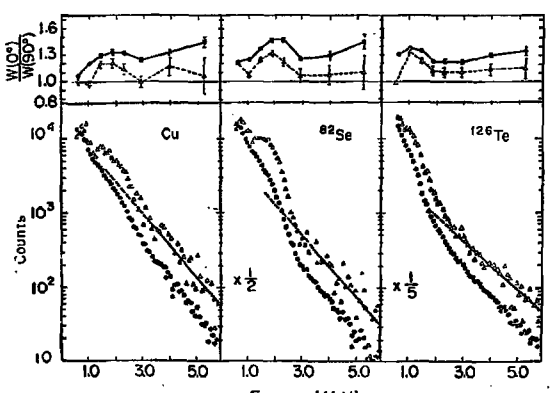

Fig.4. The raw (dots) and unfolded (triangles) gamma-rays energy spectra for compound nuclei obtained with 183 MeV Ar ions on Cu, So and Te targets (ref.19). The straight lines show the maximum part attributed to the statistical cascade. The upper plots show the 0°/90° intensity ratios.

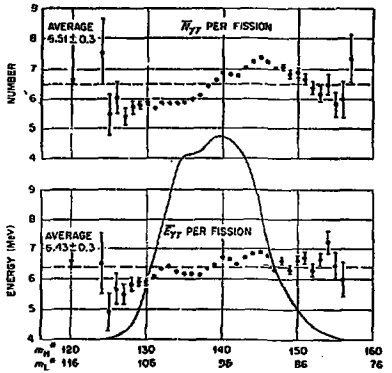

Fig.5. The average total energy $\bar{E}_{\gamma T}$ and average total number $\bar{N}_{\gamma T}$ of gamma-rays emitted per fission as functions of complementary mass pairs, in the thermal neutron induced fission of ^{235}U. The thin solid line is the fragment mass distribution. From ref.22 .

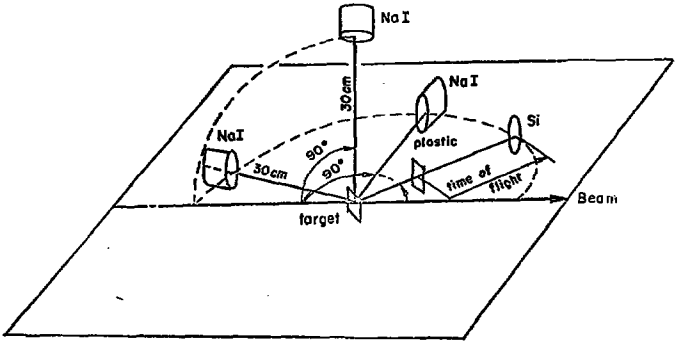

Fig.6. Schematic arrangement of detectors of fragments and coincident gamma-rays in the experiments of ref.31.

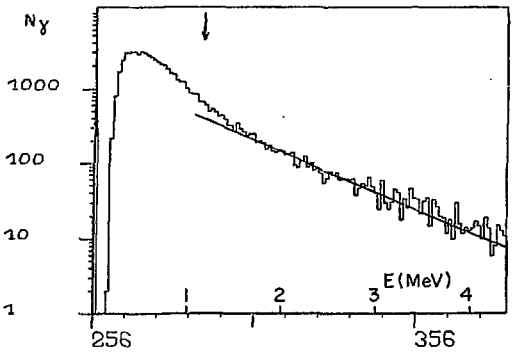

Fig.7. Cu+Au reactions at 443 MeV. γ spectrum coincident with quasi-fission fragments detected at 35°. The arrow indicates the theoretical maximum Yrast energy

from Ref.31,42.

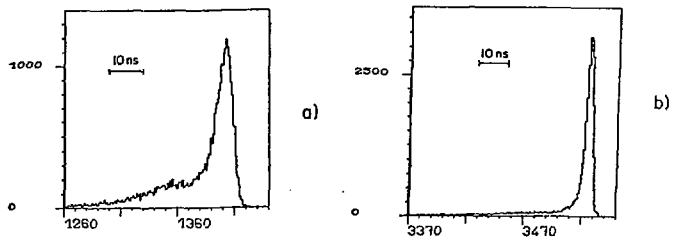

Fig.8. Time differences between the light fragments and the NaI detectors. Besides the γ-rays peaks present at all angles, a broad contribution of neutrons is present at direction a) close to that of the fragment. This contribution is much weaker at direction b) 60° from the fragment direction. System 443 MeV Cu+Au. From Ref.31,42.

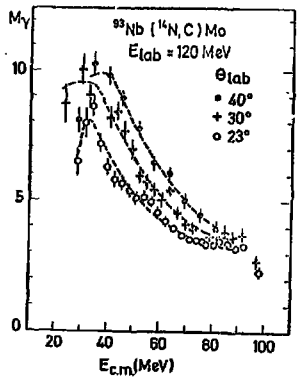

Fig.9. System $^{14}N+^{93}Nb$ at 120 MeV. Gamma-ray multiplicity versus the final kinetic energy of C at 3 angles. From Ref.30.

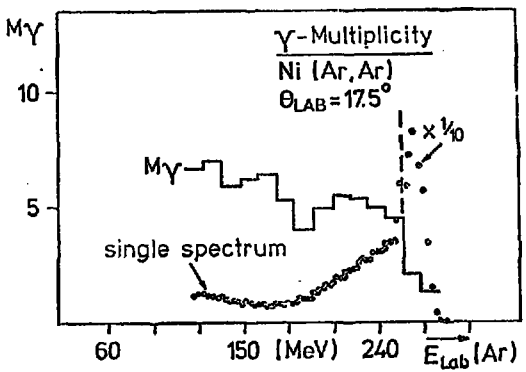

Fig.10. System $^{40}Ar+^{58}Ni$ at 280 MeV. Gamma-ray multiplicity versus the final kinetic energy of final fragments of Z equal to that of the projectile. The distribution of these fragments is indicated by the dots. From Ref.29.

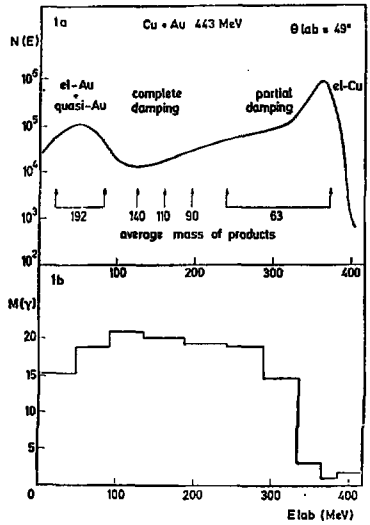

Fig.11. System $^{63}Cu+^{197}Au$ at 443 MeV. a : energy spectrum (log.scale) of the fragments detected at 49°. The arrows indicate the average mass associated with the kinetic energy scale. b : corresponding average γ-ray multiplicity. The relative uncertainties are < 2%. From Ref.31.

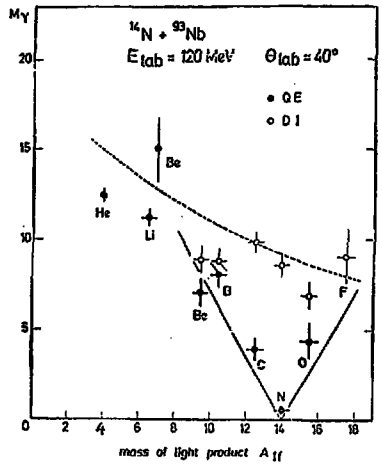

Fig.12. System $^{14}N+^{93}Nb$ at 120 MeV. Open points : γ-ray multiplicity of light DIC fragments versus their mass. The dashed line is calculated with the sticking hypothesis for spherical fragments assuming $\Delta\ell = 2.4\ \hbar$ (the dots are relative to the quasi-elastic component). From Ref.30.

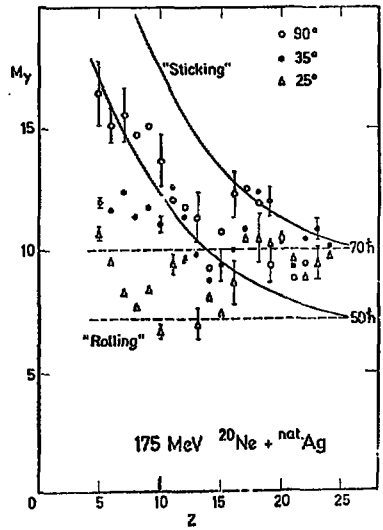

Fig.13. System $^{20}Ne+Ag_R$ at 175 MeV. Gamma-multiplicity versus Z for the relaxed component at 3 laboratory angles. The solid lines are calculated with the sticking hypothesis for $\ell_i = 70$ and 50 respectively, assuming $\Delta\ell = 2$ M_γ. The dotted lines correspond to the rolling. From Ref.32.

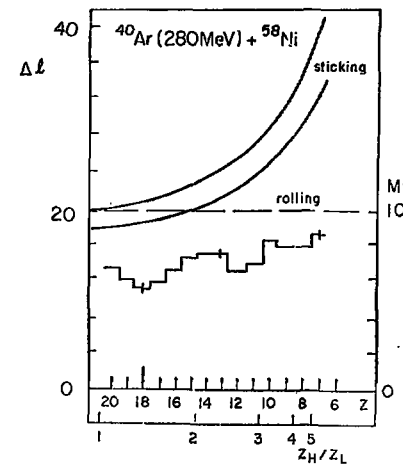

Fig.14. System $^{40}Ar+^{58}Ni$ at 280 MeV. Gamma-ray multiplicity versus Z for the relaxed component, at laboratory angles between 16° and 32°. The solid lines are calculated with the sticking hypothesis (for spherical and prolate fragments, see fig.2) for $\ell_i = 70$ assuming $\Delta\ell = 2$ M_γ . Data from Ref.29.

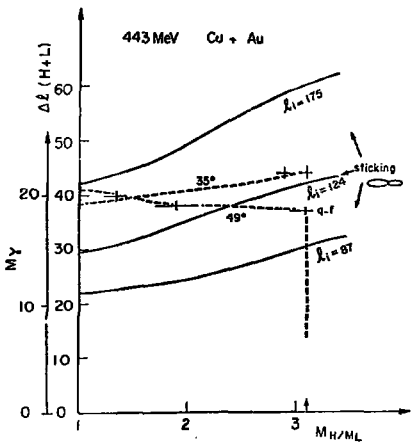

Fig.15. System $^{63}Cu+^{197}Au$ at 443 MeV. Gamma-ray multiplicity versus the fragment mass ratio for the quasi-fission component, at 2 laboratory angles (dashed lines). The solid lines are calculated with the sticking hypothesis for prolate fragments (minimal deformation deduced from the measured kinetic energy) for ℓ_i=175 (maximum ℓ-value contributing to relaxed DIC), 124 (average value if ℓ_{CF}=0) and 87 (175/2). $\Delta\ell = 2M_\gamma$. Data from Ref.31.

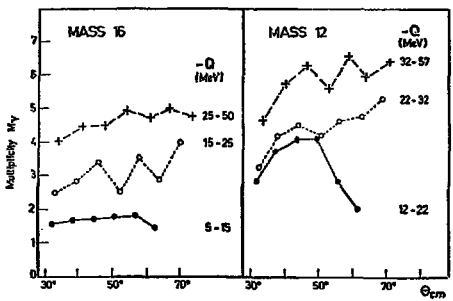

Fig.16. $^{16}O+Ni$ 96 MeV gamma-multiplicity versus center-of-mass scattering angle for mass 16 and 12 products of different Q-values. The relaxed component (triangles) stand out by having the largest M_γ. Error bars indicate statistical errors only. From Ref.28.